Mechanisms of Nonhormonal Activation of Adenylate Cyclase Based on Target Analysis†

A. S. Verkman*
Cardiovascular Research Institute, University of California, San Francisco, California 94143
D. A. Ausiello
Renal Unit, Massachusetts General Hospital, Harvard Medical School, Boston, Massachusetts 02114
C. Y. Jung
Department of Biophysics, State University of New York, Buffalo, New York 14215
K. L. Skorecki
Division of Nephrology, Toronoto General Hospital, University of Toronto, Toronto, Ontario, Canada M5G1L7
Received December 13, 1985; Revised Manuscript Received March 3, 1986

ABSTRACT: Radiation inactivation was used to examine the mechanism of activation of adenylate cyclase in the cultured renal epithelial cell line LLC-PK_1 with hormonal (vasopressin) and nonhormonal (GTP, forskolin, fluoride, and chloride) activating ligands. Intact cells were frozen, irradiated at −70 °C (0–14 Mrad), thawed, and assayed for adenylate cyclase activity in the presence of activating ligands. The ln (adenylate cyclase activity) vs. radiation dose relation was linear (target size 162 kDa) for vasopressin- (2 μM) stimulated activity and concave downward for unstimulated (10 mM Mn^{2+}), NaF- (10 mM) stimulated, and NaCl- (100 mM) stimulated activities. Addition of 2 μM vasopressin did not alter the ln activity vs. dose relation for NaF- (10 mM) stimulated activity. The dose–response relations for adenylate cyclase activation and for transition in the ln activity vs. dose curve shape were measured for vasopressin and NaF. On the basis of our model for adenylate cyclase subunit interactions reported previously [Verkman, A. S., Skorecki, K. L., & Ausiello, D. A. (1986) *Am. J. Physiol. 260*, C103–C123] and of new mathematical analyses, activation mechanisms for each ligand are proposed. In the unstimulated state, equilibrium between $\alpha\beta$ and $\alpha + \beta$ favors $\alpha\beta$; dissociated α binds to GTP (rate-limiting step), which then combines with the catalytic (C) subunit to form active enzyme. Vasopressin binding to receptor provides a rapid pathway for GTP binding to α. GTP and its analogues accelerate the rate of α_{GTP} formation. Forskolin inhibits the spontaneous deactivation of activated C. Activation by fluoride may occur without $\alpha\beta$ dissociation or GTP addition through activation of C by an $\alpha\beta$–F complex.

Adenylate cyclase plays a central role in the regulation of cellular metabolism and in the transduction of signals carried by circulating hormones and neurotransmitters. The adenylate cyclase enzyme consists of at least four subunits that are required for hormone stimulation of enzyme activity (Rodbell, 1980; Ross & Gilman, 1980; Stiles et al., 1984). The precise sequence of subunit interactions is now known by which activation of the catalytic subunit occurs in response to hormone binding to the receptor subunit. In addition to stimulation by hormone, a number of nonhormonal activators of adenylate cyclase, which do not require involvement of the receptor subunit, have been identified including fluoride, chloride, forskolin, and GTP.[1]

We have used the radiation-inactivation method to examine the subunit interactions of adenylate cyclase in intact, cultured renal epithelial cells (LLC-PK_1). Previously, we developed a biophysical model to interpret nonlinear ln activity vs. radiation dose curves (Verkman et al., 1984, 1986) and proposed a mechanism for the sequence of subunit interactions of adenylate cyclase based on measured ln (adenylate cyclase activity) vs. dose curves obtained in the unstimulated states (Skorecki et al., 1986). The proposed mechanism for stimulation of adenylate cyclase by hormone included dissociation of the guanine nucleotide regulatory subunit into α and β subunits, a direct effect of hormone to accelerate GTP addition to the α subunit, and a coupling reaction between α_{GTP} and the catalytic subunit (C) to form active enzyme (C*).

In this paper we use the radiation-inactivation technique to examine further the mechanism of activation of adenylate cyclase by nonhormonal activators and the dose–response relations for activation of adenylate cyclase by vasopressin. A new approach to study complex reaction mechanisms with radiation inactivation is used in which changes in ln activity vs. dose curves shape are detected from the dose–response relations of activating ligands obtained at a zero and a single nonzero radiation dose. On the basis of the experimental data, specific models for the activation of adenylate cyclase by vasopressin, fluoride, chloride, GTP, and forskolin are presented.

† This work was supported by NIH Grants AM35124, AM19406, and AM30410, Ontario Heart Foundation Grant AN106, a Kidney Foundation of Canada grant, and grants from the UCSF Academic Senate, MSC Clough Fund, and Hedco Foundation.
* Address correspondence and requests for reprints to this author.

[1] Abbreviations: α and β, subunits of the guanyl nucleotide regulatory protein; G, guanyl nucleotide regulatory protein; R, receptor subunit; C, catalytic subunit; GTP, guanosine 5′-triphosphate; GDP, guanosine 5′-diphosphate; Gpp(NH)p, 5′-guanylyl imidodiphosphate; cAMP, adenosine cyclic 3′,5′-monophosphate; Tris-HCl, tris(hydroxymethyl)aminomethane hydrochloride; EDTA, ethylenediaminetetraacetic acid; EGTA, ethylene glycol bis(β-aminoethyl ether)-*N,N,N′,N′*-tetraacetic acid.

0006-2960/86/0425-4566$01.50/0

Materials and Methods

Materials. Cell culture media, sera, and enzymes were obtained from Gibco (Grand Island, NY). ATP, cAMP, GTP, adenosine deaminase, creatine kinase, and creatine phosphate were obtained from Boehringer-Mannheim (Indianapolis, IN). [^{32}P]ATP and [^{3}H]cAMP were obtained from New England Nuclear (Bedford, MA). All other chemicals were of reagent grade and were obtained from Sigma Chemical Co. (St. Louis, MO).

Cell Culture. LLC-PK$_1$ cells (ATC NO CL-101) were grown to confluency in 35-cm^2 plastic culture dishes in Dulbecco's modified Eagle's medium supplemented with 10% fetal bovine serum as described previously (Roy & Ausiello, 1981).

Radiation Inactivation. Cells were washed in phosphate-buffered saline, frozen in liquid N_2, and stored in dry ice prior to and following radiation. Frozen cells were radiated under flowing liquid N_2 with a 0.5-mA beam of 1.5-MeV electrons generated from a Van de Graaf accelerator. Temperature was maintained at −45 to −55 °C at all times. Dosimetry was performed with Blue Cellophane foil [Du Pont, dimethoxydiphenylbisazobis(8-amino-1-naphthol-5,7-disulfonic acid)] and calibrated against exogenous and endogenous markers as described previously (Skorecki et al., 1986; Venter et al., 1983).

Enzyme Assay. Adenylate cyclase activity was assayed as described previously (Ausiello & Hall, 1981). Thawed cells were scraped in 5 mM Tris-HCl and 2 mM EDTA, pH 7.4, disrupted with 15 strokes of a Dounce homogenizer, and centrifuged at 50g for 10 min to remove whole cells and nuclei. The supernatant was centrifuged at 10000g, and the pellet was resuspended in 5 mM Tris-HCl and 0.5 mM EGTA, pH 7.4. Adenylate cyclase activity was assayed by measuring the rate of conversion of [^{32}P]ATP to [^{32}P]cAMP over a 20-min period where cAMP generation was linear. Incubation medium consisted of 50 mM Tris-HCl, 0.2 mM EGTA, 0.1 mM cAMP, 0.1 mM ATP, 5 mM $MgCl_2$, 0.5 mg/mL creatine kinase, 1.5 mg/mL creatine phosphate, 3 μg/mL adenosine deaminase, 10–20 μCi/mL [^{32}P]ATP, and specified concentrations of activating ligands in a final volume of 50 μL per assay tube containing 15–20 μg of homogenate protein. [^{32}P]cAMP was measured as described previously. Activity was expressed as pmol of cAMP (mg of protein)$^{-1}$ (20 min)$^{-1}$.

Calculations. In each experiment 10–20 separate dishes were radiated, each at a different radiation dose including zero radiation. Adenylate cyclase activities were determined in the membrane particulate fractions prepared from each dish in triplicate. For ln activity vs. radiation dose plots, activity was expressed as a fraction of activity in the nonradiated sample.

For vasopressin-stimulated adenylate cyclase activity, the ln activity vs. dose relation was fitted to a line. The slope of the line is related to the target size (m) by the relation m = 640 kDa × slope (in Mrad^{-1}) (Venter et al., 1983; Kempner & Schlegel, 1979). For concave downward ln activity vs. radiation dose curves, data were fitted to a simple subunit dissociation model described previously (Skorecki et al., 1986):

$$\ln \text{activity} = b + \ln \frac{[(e^{-D/D_0} + K_b)^2 + 4K_b e^{-D/D_0}]^{1/2} - e^{-D/D_0} - K_b}{[(1 + K_b)^2 + 4K_b]^{1/2} - 1 - K_b} \quad (1)$$

where the fitted parameters are K_b, a dimensionless dissociation constant, b, the intercept on the ln activity axis at zero radiation dose, and D_0 (in Mrad), which is related to the limiting slope of the ln activity vs. dose relation at high radiation dose. Data were fitted to eq 1 with a weighted nonlinear fitting procedure. Equation 1 was found to be the simplest empiric equation that described the data well, had direct physical meaning, and required only a three-parameter fit.

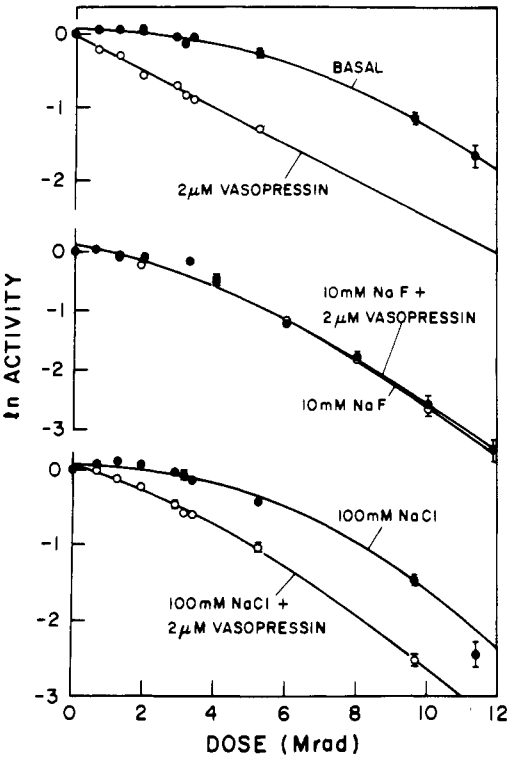

FIGURE 1: Radiation inactivation of adenylate cyclase in the basal and activated states. Adenylate cyclase activity was assayed in triplicate at each radiation dose in membrane particulate fractions prepared from radiated cells. Activity at each dose was expressed as a fraction of activity in the nonradiated sample. Error bars represent 1 SD. Activating ligands (NaF, NaCl, vasopressin) were added to the membrane particulate fractions after radiation. Data at 2 μM vasopressin were fitted to a linear inactivation model with a target size of 162 ± 5 kDa. Remaining curves were fitted to the model given in eq 1. Fitted parameters: (Basal) D_0 = 2.4 ± 0.2 Mrad, K_b = 0.03 ± 0.01, and b = 0.6 ± 0.4; (NaF + vasopressin) D_0 = 2.3 ± 0.1 Mrad, K_b = 0.27 ± 0.1, and b = 0.1 ± 0.1; (NaF) D_0 = 2.3 ± 0.1 Mrad, K_b = 0.25 ± 0.1, and b = 0.1 ± 0.1; (NaCl) D_0 = 2.1 ± 0.2 Mrad, K_b = 0.03 ± 0.02, and b = 0.06 ± 0.04; (NaCl + vasopressin) D_0 = 2.5 ± 0.2, K_b = 0.5 ± 0.2, and b = 0.05 ± 0.03. Adenylate cyclase activity in the nonradiated samples were [in pmol (mg of protein)$^{-1}$ (20 min)$^{-1}$]: 306 (basal), 1820 (vasopressin), 3490 (NaF + vasopressin), 3180 (NaF), 2582 (NaCl + vasopressin), and 482 (NaCl).

The dose–response curves for activation of adenylate cyclase by activating ligands were fitted to a single-site model:

$$A([L]) = A_1 + A_2[L]/(K_a + [L]) \quad (2)$$

where [L] is ligand concentration, $A([L])$ is measured activity, A_1 is activity at [L] = 0, $A_1 + A_2$ is maximum activity, and K_a is a single-site dissociation constant.

For experiments involving ligand concentration–response relations at a single radiation dose, the ratios of activities of the radiated to the nonradiated samples for a series of ligand concentrations were fitted to the single-site model given in eq 2.

Results

Inactivation Curve Shape Studies. Figure 1 shows the ln activity vs. radiation dose curve shapes for adenylate cyclase activity measured in the basal (unstimulated) state and in the presence of several activating ligands. In the basal state, the ln activity vs. dose curve is concave downward, similar to data reported previously (Skorecki et al., 1986). In the presence of 2 μM vasopressin added after radiation exposure and sample thawing, the ln activity vs. dose curve becomes linear with a target size of 162 kDa, consistent with previously reported target sizes of 172 ± 6 kDa (n = 11, SEM) for similar ex-

periments and 166 ± 8 kDa (n = 6) for experiments in which 2 μM vasopressin was added both prior to and after radiation exposure. We previously reported that 100 μM forskolin also resulted in transition from the concave downward to linear ln activity vs. dose relations with a target size of 163 ± 27 kDa (n = 3).

As shown in Figure 1, activation of adenylate cyclase by 10 mM NaF results in a concave downward ln activity vs. dose relation, with slightly less curvature than that observed for the basal state. In six measured ln activity vs. dose relations at 10 mM NaF, the apparent target size for adenylate cyclase, calculated from the slope of the ln activity vs. dose curve between 10 and 15 Mrad, was 225 ± 22 kDa (SEM). This value is significantly greater than the apparent target size for adenylate cyclase measured in the basal state (169–196 kDa) and with stimulation by vasopressin or the nonhormonal activators forskolin and Gpp(NH)p (168 ± 4 kDa). Surprisingly, ln activity vs. dose curves obtained with stimulation of adenylate cyclase by 10 mM NaF + 2 μM vasopressin were not different from those obtained by stimulation with 10 mM NaF alone. Possible reasons for the loss of ability of vasopressin to cause a transition in the ln activity vs. dose curve shape from concave downward to linear in the presence of NaF are discussed under Model. In analogy to NaF, 100 mM NaCl results in activation of adenylate cyclase without linearization of the ln activity vs. dose relation; addition of 2 μM vasopressin results in partial linearization of the curve.

The activity–dose relation for activation of adenylate cyclase by vasopressin is examined in Figure 2. In a nonradiated sample, the activity vs. dose curve is fitted well to a single-site model with a Hill coefficient of unity and a vasopressin single-site dissociation constant K_a of 0.5 nM. In four sets of experiments, the vasopressin K_a was 0.5 ± 0.2 nM (SEM).

It is interesting that the activation constant is significantly lower than the maximum equilibrium affinity for vasopressin binding to intact LLC-PK$_1$ cells (12 nM) or to membrane particulate fractions prepared from the cells (5–10 nM) (Roy & Ausiello, 1981). In order to explore the mechanism for this nonlinear coupling between receptor occupancy and enzyme activation, the dose–response relation for vasopressin linearization of the ln (activity) vs. radiation dose curve was measured. Experimentally, we made several attempts to generate a series of ln activity vs. dose curves for adenylate cyclase stimulated by intermediate vasopressin concentrations between 0 and 2 μM. Because of interexperiment variation, it was not possible to resolve consistently small variations in the curve shape between fully concave downward and linear. A direct method that did resolve small differences in curve shape was to study the dependence of fractional adenylate cyclase inactivation at a single radiation dose on vasopressin concentration.

The rationale for this experimental approach is based on the theory for radiation inactivation of multimeric enzymes described previously (Verkman et al., 1986). In a "dissociative model", where addition of activating ligand causes dissociation of a subunit complex to form an active monomeric subunit, transition from a curved to linear ln activity vs. dose relation occurs. The theory predicts that curves drawn at different ligand concentrations do not overlap; therefore, measurement of the fractional inactivation at a single radiation dose is a good approximation of the overall curve shape, particularly at high radiation doses, where the ln activity vs. dose curve is nearly linear.

For vasopressin stimulation of adenylate cyclase (Figure 2, bottom), the vasopressin concentration at which "half-linearization" of the ln activity vs. dose relations occurs is ~0.4 nM, similar to the K_a for vasopressin activation of adenylate cyclase but dissimilar to the equilibrium affinity for vasopressin binding to its receptor.

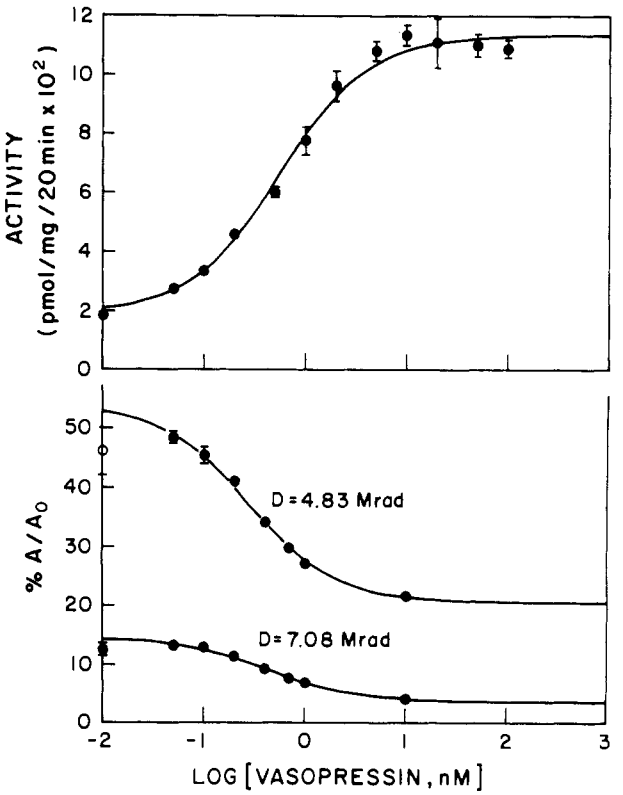

FIGURE 2: Dose–response relations for activation of adenylate cyclase by vasopressin. Adenylate cyclase activity was determined in triplicate as a function of vasopressin concentration in samples radiated with 0-, 4.83-, and 7.08-Mrad doses. (Top) Activity in the nonradiated sample was fitted to the model given in eq 2 with A_1 = 930 ± 20 pmol (mg of protein)$^{-1}$ (20 min)$^{-1}$, A_2 = 1.9 ± 0.1 pmol (mg of protein)$^{-1}$ (20 min)$^{-1}$; and K_a = 0.51 ± 0.06 nM. (Bottom) Activities are expressed as a percentage of the activity in the nonradiated sample (% A/A_0). Fitted parameters with eq 2 were as follows: (4.83 Mrad) A_2 = −33 ± 2%, A_1 = 54 ± 2%, and K_a = 0.28 ± 0.04 nM; (7.08 Mrad) A_2 = 10.9 ± 0.4%, A_1 = 14.5 ± 0.4%, and K_a = 0.43 ± 0.05 nM.

The dose–response relations for activation of adenylate cyclase by NaF are shown in Figure 3. Half-maximal activation of adenylate cyclase occurs at ~6 mM NaF, whereas the half-point for relative inactivation at a single radiation dose occurs at an order of magnitude lower concentration. This discrepancy in concentrations supports the quite different proposed mechanism of activation of adenylate cyclase by fluoride as compared to vasopressin (see Model).

Model

On the basis of the ln (adenylate cyclase activity) vs. radiation dose curve shapes for the basal and vasopressin-stimulated states, we have previously examined a series of mechanisms for the sequence of subunit interactions by which hormone–receptor binding results in adenylate cyclase activation (Verkman et al., 1986). The proposed mechanism that was consistent with radiation inactivation data, as well as vasopressin binding data, is the cyclic dissociation model shown in eq 3. The adenylate cyclase subunits are α, β, R (receptor), and C (catalytic). The subscripts D and T refer to bound GDP and GTP, respectively. H is vasopressin, C* represents active enzyme. Bimolecular equilibrium dissociation constants are K_β, K_C, K_H, K_{HR}, and K_{HR}'; unimolecular rate constants are

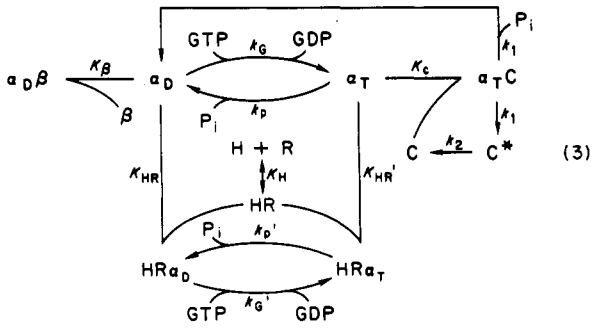

k_G, k_G', k_p, k_p', k_1, and k_2 as defined previously (Verkman et al., 1986).

In the basal state ([H] = 0), the rate-limiting reaction of GTP with α_D is slow, resulting in low activity. In the presence of vasopressin, there is a rapid alternate pathway for GTP addition to α_D ($HR\alpha_D \rightarrow HR\alpha_T$), which results in increased activity ([C*]) and dissociation of $\alpha_D\beta$. Although the model in eq 3 was developed from experiments on vasopressin activation of adenylate cyclase in cultured renal epithelial cells, the proposed sequence of subunit interactions required for activation may also apply to other hormone–adenylate cyclase systems such as the β-adrenergic and glucagon receptor systems. This model has many of the features proposed for adenylate cyclase activation in the β-adrenergic system, including $\alpha\beta$ dissociation, rate-limiting GTP binding, and activation of the catalytic subunit by a collision coupling mechanism (Tolkovsky et al., 1972; Stiles et al., 1984). Although the model can account for activation of adenylate cyclase by a variety of hormonal and nonhormonal ligands, it does not include the inhibitory guanyl regulatory subunit (N_i) and therefore cannot be used to test hypotheses concerning inhibitory ligands.

In the absence of vasopressin or of the R subunit, adenylate cyclase activation may occur by variations in rate constants (k_G, k_p, k_1, k_2) due to the presence of nonhormonal activators or by an entirely different mechanism. Figure 4 shows the dependences of relative adenylate cyclase activity on each of the four rate constants. The parameters used for the simulation are given in the legend to Figure 4; although the detailed curve shapes are parameter-dependent, the qualitative features of the curves are not. Increasing k_G, as would be expected with increasing [GTP], accelerates the reaction of GTP addition to α_D in analogy to the hormone-dependent mechanism of adenylate cyclase activation. Increasing k_1 or decreasing k_2 also results in enzyme activation by allowing a greater fraction of total C to exist as C*. There is a small decrease in enzyme activity with increasing k_p, due to a nonactivating pathway for α_T hydrolysis, which becomes marked when k_p becomes greater than 100 (not shown). A feature of the mechanism for activation of adenylate cyclase by increasing k_G or decreasing k_p is that increased activity is directly associated with $\alpha_D\beta$ dissociation through mass action. Activation of adenylate cyclase by increasing k_1 or decreasing k_2 primarily alters the fraction of C present as C*, with a secondary effect on $\alpha_D\beta$ dissociation.

The ln activity vs. dose curves predicted as a function of the four rate constants are shown in Figure 5. Activation of adenylate cyclase by increasing k_G or decreasing k_2 results in a transition from a concave downward to a linear inactivation curve. However, activation by decreasing k_p or increasing k_1 is associated with increased downward curvature of the ln activity vs. dose plot. On the basis of the curves shown in Figures 4 and 5, the values of the rate constants at which half-maximal activation occurs (Figure 4) and at which there

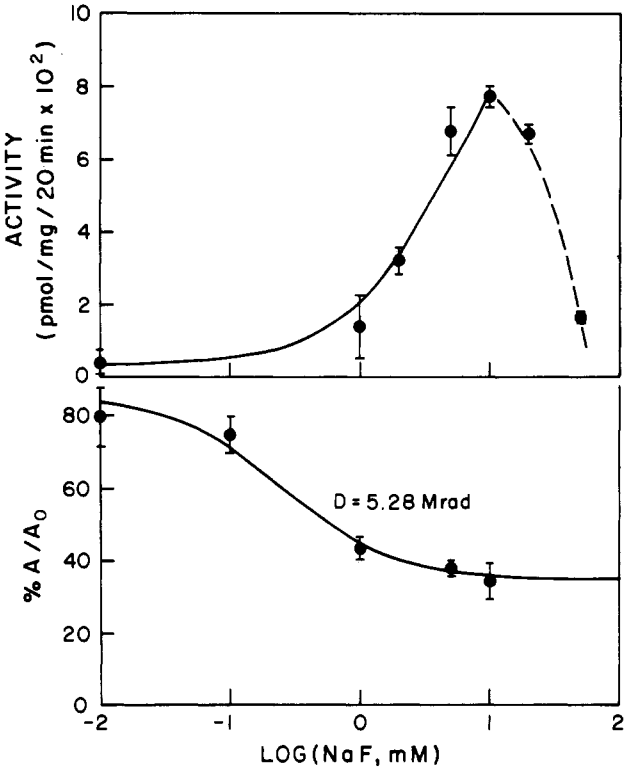

FIGURE 3: Dose–response relations for activation of adenylate cyclase by fluoride. Adenylate cyclase activities were determined in triplicate as a function of NaF concentration at 0- and 5.28-Mrad radiation doses. (Top) Fitted parameters were A_2 = 1700 ± 200 pmol (mg of protein)$^{-1}$ (20 min)$^{-1}$, A_1 = 0.3 ± 0.4 pmol (mg of protein)$^{-1}$ (20 min)$^{-1}$, and K_a = 6 ± 3 mM. Adenylate cyclase activity decreased for [NaF] > 10 mM. (Bottom) Adenylate cyclase activity is expressed as a ratio of activity of the radiated sample to activity of the nonradiated sample at each NaF concentration. Fitted parameters were A_2 = −51 ± 6%, A_1 = 85 ± 6%, and K_a = 0.26 ± 0.1 mM.

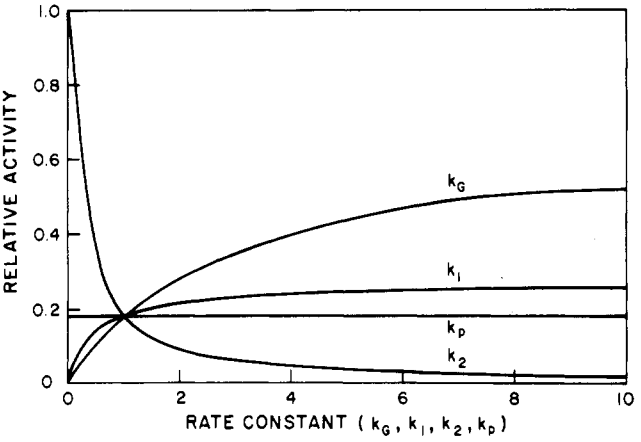

FIGURE 4: Nonhormonal mechanisms of adenylate cyclase activation: effect of rate constants on activity. Effects of varying the rate constants k_1, k_2, k_G, and k_p on adenylate cyclase activity were calculated for the model given in eq 3. For each computer-simulated curve, the parameters were K_β = 0.1, K_C = 0.001, α_T = 1, β_T = 1, and C_T = 1. Three of the four rate constants were set equal to 1, and the fourth rate constant was varied between 0 and 10. The maximum possible adenylate cyclase activity was achieved when relative activity = 1, in which all C is in the C* form.

is "half" transition between concave downward and linear inactivation curve shape are similar for k_G, k_1, and k_2.

We have also examined the effects of variations in K_β and K_C on enzyme activity and inactivation curve shape. Through mass action, increasing K_β or decreasing K_C results in enzyme activation. Activation by increasing K_β results in transition from concave downward to linear inactivation curve shape,

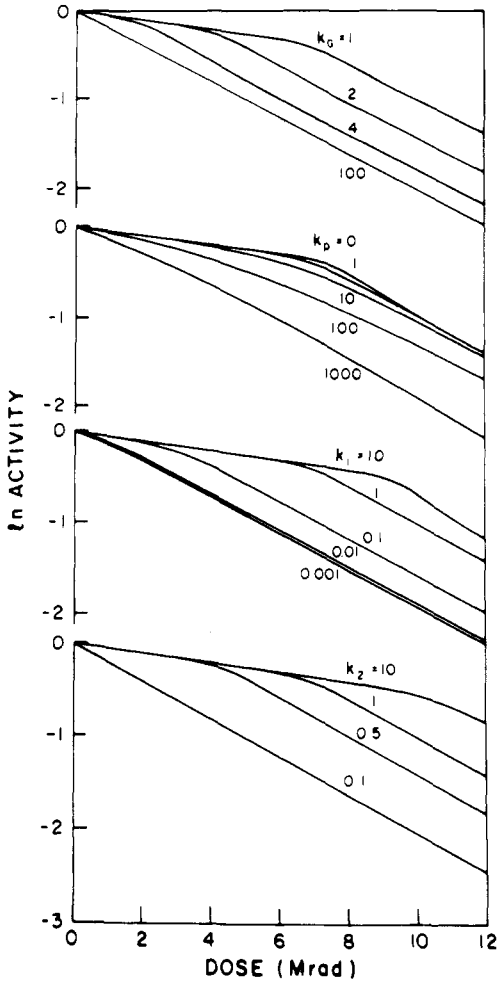

FIGURE 5: Nonhormonal mechanisms of adenylate cyclase activation: target analysis curve shapes. The predicted ln activity vs. radiation dose curve shapes for the model in eq 3 were calculated. Molecular weights are 45 (α), 35 (β), and 130 kDa (C). The remaining parameters are the same as those given in the legend to Figure 4. For each set of curves, one of the rate constants is varied while the remaining rate constants are held fixed at unity.

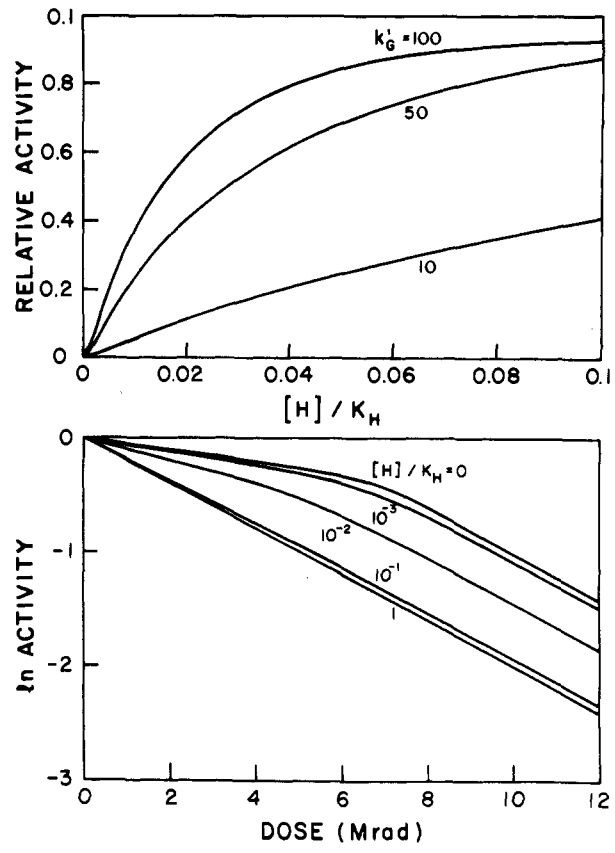

FIGURE 6: Activation of adenylate cyclase by hormone. Adenylate cyclase activities were calculated for the model given in eq 3 with $K_\beta = 0.1$, $K_C = 0.001$, $K_{HR} = 1$, $K_{HR}' = 1$, $k_1 = 1$, $k_2 = 1$, $k_G = 1$, and $k_P = 1$. (Top) The adenylate cyclase activity is calculated as a function of $[H]/K_H$ for several values of k_G'. (Bottom) The predicted radiation inactivation curve shapes are calculated with the parameters above, $k_G' = 100$, and a molecular weight for R of 100 kDa.

whereas activation by decreasing K_C causes the opposite transition. These qualitative results are also predictable from the principles of "associative" and "dissociative" models described previously (Verkman et al., 1986). An associative model, which has the characteristic of linear to concave downward inactivation curve shape transition with increasing activity, is one in which activating ligand causes association between subunits. In a dissociative model, the reaction step altered by activating ligand is one in which subunit dissociation occurs.

Stimulation of adenylate cyclase by GTP and its analogues is associated with transition in inactivation curve shape from concave downward to linear (Skorecki et al., 1986). The rate constant k_G is a pseudo-first-order rate constant that depends upon GTP concentration, $k_G = k_G^0[GTP]$, where k_G^0 is a concentration-independent second-order rate constant. As shown in Figures 4 and 5, increased k_G results in both adenylate cyclase activation and in a transition from concave downward to linear inactivation curve shape as found experimentally. Irreversible GTP analogues, which lock α in its activated form (α_T), would also linearize the inactivation curve because of increased $\alpha\beta$ dissociation.

Forskolin stimulation of adenylate cyclase is also associated with linearization of the inactivation curve shape. It is known that forskolin can stimulate the catalytic subunit in the absence of R, α, and β subunits (Seamon et al., 1981; Wong & Martin, 1983). On the basis of the discussion in this section, decreases in k_2 cause both adenylate cyclase activation and linearization of the inactivation curve shape. Decreased k_2 indicates prolongation of the activated C* state. By prolonging the state of activated C*, forskolin would be expected to augment the effect of other ligands (such as hormone) that act at distinct and more proximal steps in the activation sequence. Indeed, this has been described in a number of systems (Seamon & Wetzel, 1984), and we have confirmed additivity of forskolin-plus vasopressin-stimulated adenylate cyclase activities in the LLC-PK_1 membrane system (data not shown).

Recent studies of Bouhelal et al. (1985) have shown an increase in the sedimentation coefficient for the catalytic subunit in the presence of forskolin, consistent with stabilization of an αC complex. On the basis of results given above, other possible interactions of forskolin with the subunits of adenylate cyclase that would cause both enzyme activation and linearization of the inactivation curve shape would be forskolin-related increases in k_G and K_β. However, effects of forskolin on these parameters exclusively could not account for the measured activation of resolved C by forskolin (Bender et al., 1984). Furthermore, additivity of forskolin with other activating ligands for stimulation of adenylate cyclase would not be predicted for these mechanisms.

The characteristics of hormone-stimulated adenylate cyclase activity are shown in Figure 6. Relative activity is a saturating function of $[H]/K_H$; the value of $[H]/K_H$ at half-maximal activity decreases with increasing k_G'. It is clear that the coupling relation between receptor occupancy and enzyme

activation is strongly dependent on the ratio k_G'/k_G. The ln activity vs. dose curves were drawn with $k_G = 100$. Both half-maximal activity and half-transition from concave downward to linear inactivation curve shape occur at $[H]/K_H \sim 0.01$. In general, the model in eq 3 predicts that the K_a for hormone activation (eq 3) should be very similar to K_a for transition in inactivation curve shape, rather than to the equilibrium constants (K_H, K_{HR}, K_{HR}'), that define hormone binding to receptor. This prediction was found to be the case for vasopressin stimulation of adenylate cyclase as given in Figure 2.

As discussed above, the mechanism of adenylate cyclase activation by vasopressin, forskolin, GTP, and GTP analogues is understandable in terms of the basic model given in eq 3. However, the mechanism by which fluoride and possibly chloride activate adenylate cyclase may be quite different. As shown in Figure 1, 10 mM NaF increases adenylate cyclase activity 10-fold without linearizing the inactivation curve. Addition of 2 μM vasopressin has no effect on the inactivation curve shape. The target size for adenylate cyclase (225 ± 22 kDa) stimulated by NaF (10 mM) is significantly greater than that for stimulation by Mn^{2+}, vasopressin, Gpp(NH)p, or forskolin (163–172 kDa), suggesting that the subunit structure required for adenylate cyclase activation by fluoride is different from that required for activation by the other ligands. In addition, the change in inactivation curve shape by NaF (Figure 3, bottom) occurs at <1 mM NaF, before significant activation of adenylate cyclase activation has occurred (Figure 3, top). These observations cannot be accommodated by the model in eq 3 and suggest that activation of adenylate cyclase by NaF occurs by a different mechanism.

The model in eq 3 predicts that the measured adenylate cyclase target size for activation by any ligand is equal to the sum of molecular weights of the α and C subunits. The best recent estimates for molecular weights of α and C are 45 and 140 kDa (Sternweis et al., 1981; Bender et al., 1984; Smigel et al., 1984), which give a composite molecular weight (184 kDa) similar to the measured adenylate cyclase target sizes for stimulation by Mn^{2+}, vasopressin, Gpp(NH)p, and forskolin but less than that for NaF stimulation ($P < 0.01$). The β subunit has a molecular weight of 35 kDa. We suggest the following as a possible model for simulation of adenylate cyclase by NaF without $\alpha\beta$ dissociation:

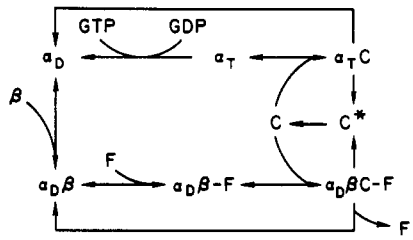

(4)

According to this model, increasing NaF results in formation of $\alpha_D\beta$C–F, which can dissociate into active C*. It is indeed known that neither R nor GTP is requires for fluoride activation of adenylate cyclase (Sternweis & Gilman, 1982). The target size predicted for maximal NaF stimulation for the model in eq 4 is equal to the composite $\alpha\beta$C molecular weight, 219 kDa; the predicted inactivation curve shape for this model is shown in Figure 7. For the parameters chosen to carry out the data simulation, NaF-stimulated adenylate cyclase activity results in a concave downward inactivation curve that is not linearized with vasopressin, similar to the data in Figure 1. The curve drawn for 2 μM vasopressin is linear and less steep than the NaF and NaF + vasopressin curves.

These results suggest a mechanism for adenylate cyclase

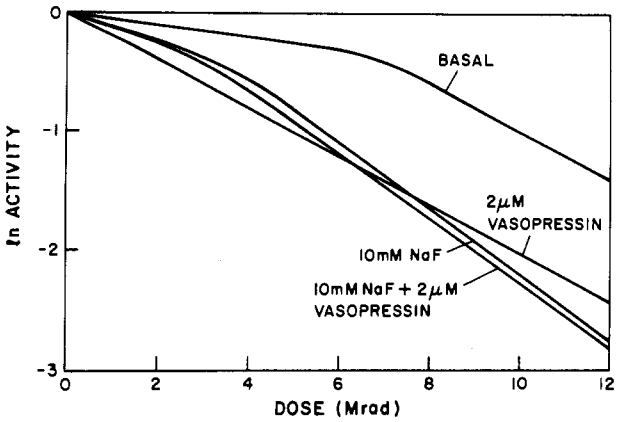

FIGURE 7: Model for activation of adenylate cyclase by fluoride. The radiation-inactivation curve shapes are calculated for the model given for fluoride activation of adenylate cyclase in eq 4. Steady-state C* concentrations were calculated as a function of radiation dose from subunit molecular weights, stoichiometries, equilibrium constants, and rate constants by an iterative procedure given previously in the appendix to Verkman et al. (1986). Parameters are the same as those given in the legends to Figures 5 and 6 with $K_F = 1$ mM, $K_{HF} = 0.001$, and $k_3 = 1$. K_F and K_{HF} are dissociation constants defined by the relations: $K_F = [F][\alpha_D\beta]/[\alpha_D\beta\text{–}F]$ and $K_{HF} = [C][\alpha_D\beta\text{–}C]/[\alpha_D\beta C\text{–}F]$. k_3 is the rate constant for conversion of $\alpha_D\beta C$–F to C*.

activation by fluoride in the intact membrane environment that differs from mechanisms proposed previously on the basis of studies using detergent-solubilized guanyl nucleotide regulatory protein (G). These latter studies have shown a decrease in the size of solubilized G, on the basis of sedimentation parameters, upon addition of fluoride with its cofactor aluminum (Sternweis et al., 1981; Sternweis & Gilman, 1982), as well as accelerated reversal of AlF activation of G with the addition of the resolved β subunit (Northup et al., 1983). On the basis of these observations, the authors concluded that fluoride activation of detergent-solubilized G involves $\alpha\beta$ dissociation (Smigel et al., 1984a,b). It should be noted, however, that for these studies stability of resolved G could only be achieved with solubilization and purification done in the presence of fluoride. More recently, studies of Codina and co-workers (Codina et al., 1984) in which G was solubilized and purified in the absence of fluoride provided evidence for the existence of a preactivated but nondissociated state of G in the presence of added NaF. Apparent subunit dissociation in the solubilized system depended upon the detergent composition, $MgCl_2$ concentration, and temperature. However, a NaF-preactivated state of G was demonstrated to persist with subunit dissociation. Since interpretation of experiments done in solubilized systems depends upon conditions of solubilization, it is important to study the activation mechanism in the intact membrane environment. Our observations suggest that activation by fluoride occurs in the intact membrane without the necessity of $\alpha\beta$ dissociation. One possibility that is shown in eq 4 is that fluoride may bind to nondissociated $\alpha\beta$ to form a complex that can activate C.

ACKNOWLEDGMENTS

We acknowledge the technical assistance of Debbie McAnaney for enzyme assays and Charles Berenski for radiation-inactivation dosimetry.

Registry No. GTP, 86-01-1; forskolin, 66575-29-9; fluoride, 16984-48-8; chloride, 16887-00-6; vasopressin, 11000-17-2; adenylate cyclase, 9012-42-4.

REFERENCES

Ausiello, D. A., & Hall, D. (1981) *J. Biol. Chem. 256*, 9796–9798.

Bender, J. C., Wolf, L. G., & Neer, E. J. (1984) *Adv. Cyclic Nucleotide Protein Phosphorylation Res. 17*, 101-109.
Bouhelal, R., Guillon, G., Homburger, V., & Bockaert, J. (1985) *J. Biol. Chem. 260*, 10901-10904.
Codina, J., Hildebrandt, J. D., & Birnbaumer, L. (1984) *J. Biol. Chem. 259*, 11408-11418.
Kempner, E. S., & Schlegel, W. (1979) *Anal. Biochem. 92*, 2-10.
Northup, J. K., Sternweiss, P. C., & Gilman, A. G. (1983) *J. Biol. Chem. 258*, 11361-11368.
Rodbell, M. (1980) *Nature (London) 284*, 17-22.
Ross, E. M., & Gilman, A. G. (1980) *Annu. Rev. Biochem. 49*, 533-564.
Roy, C., & Ausiello, D. A. (1981) *J. Biol. Chem. 256*, 3415-3422.
Seamon, K. B., Padgett, W., & Daly, J. W. (1981) *Proc. Natl. Acad. Sci. U.S.A. 78*, 3363-3367.
Skorecki, K. L., Verkman, A. S., Jung, C. Y., & Ausiello, D. A. (1986) *Am. J. Physiol. 260*, C116-C123.
Smigel, M. D., Ross, E. M., & Gilman, A. G. (1984a) in *Cell Membranes Methods and Reviews* (Elson, E., Frazier, W., & Glaser, L., Eds.) pp 247-294, Plenum, New York.
Smigel, M. D., Katada, J., Northup, J. K., Bokoch, G. M., & Gilman, A. G. (1984b) *Adv. Cyclic Nucleotide Protein Phosphorylation Res. 17*, 1-18.
Sternweis, P. C., Northup, J. K., Smigel, M., & Gilman, A. G. (1981) *J. Biol. Chem. 256*, 11517-11526.
Stiles, G. L., Caron, M. C., & Lefkowitz, R. J. (1984) *Physiol. Rev. 64*, 661-743.
Tolkovsky, A. M., Braun, S., & Levitzki, A. (1982) *Proc. Natl. Acad. Sci. U.S.A. 79*, 213-217.
Venter, J. C., Fraser, C. M., Schaber, J. S., Jung, C. Y., Bolger, G., & Triggle, D. J. (1983) *J. Biol. Chem. 258*, 9344-9348.
Verkman, A. S., Skorecki, K. L., & Ausiello, D. A. (1984) *Proc. Natl. Acad. Sci. U.S.A. 81*, 150-154.
Verkman, A. S., Skorecki, K. L., & Ausiello, D. A. (1986) *Am. J. Physiol. 260*, C103-C114.
Wong, S. K., & Martin, B. R. (1983) *Biochem. J. 216*, 753-759.

Microtubule Assembly Is Dependent on a Cluster of Basic Residues in α-Tubulin†

Joseph Szasz,‡ Michael B. Yaffe,‡ Marshall Elzinga,§ Gregory S. Blank,‡ and Himan Sternlicht*,‡
Department of Pharmacology, Case Western Reserve University, Cleveland, Ohio 44106, and Department of Biology, Brookhaven National Laboratory, Upton, New York 11973
Received December 30, 1985; Revised Manuscript Received April 8, 1986

ABSTRACT: Previous studies have shown that tubulin, a major protein component of the microtubule, is rendered assembly incompetent when a highly reactive lysine residue (HRL) in the α polypeptide of tubulin *dimer* is reductively methylated [cf. Sherman, G., Rosenberry, T. L., & Sternlicht, H. (1983) *J. Biol. Chem. 258*, 2148-2156]. In this study we demonstrate that the HRL in bovine brain tubulin is Lys-394, a residue proximal in the α-tubulin sequence to the highly negatively charged carboxy-terminus region (residues 412-450) previously implicated in assembly. pH studies were undertaken to probe the local environment of Lys-394. These studies indicated that Lys-394 reactivity toward HCHO is sensitive to the titration of a pK_a 6.3 group presumed to be a histidine residue. This assignment is supported by our finding that histidine modification via diethyl pyrocarbonate strongly affects Lys-394 reactivity toward HCHO as well as microtubule assembly. We propose on the basis of secondary structure considerations and published sequence data for a variety of tubulins that Lys-394 is part of an evolutionarily conserved cluster of basic residues (effective charge: 2+ to 2.5+ at neutral pH) composed of Lys-394, His-393, and Arg-390, which is important for tubulin function and which renders Lys-394 reactive as a nucleophile.

Tubulin, the major protein of microtubules, is a heterodimer consisting of two polypeptide chains, α and β, each ~50 kdaltons (Luduena et al., 1977). Microtubule assembly is affected by divalent cations (Rosenfeld et al., 1976; Larsson et al.; Solomon, 1977) and basic proteins, i.e., microtubule-associated proteins (MAPs)[1] (Lee et al., 1978a,b; Scheele & Borisy, 1979). A number of these agents are thought to bind at the carboxy termini of tubulin, i.e., at residue positions ~410-451 in α polypeptide and ~400-446 in β polypeptide, which contain ~40% of all the glutamates and ~20% of all the aspartates in tubulin (Ponstingl et al., 1981; Krauhs et al., 1981; Valenzuela et al., 1981), and are presumed to affect assembly in part by modulating electrostatic interactions between carboxy termini (Maccioni et al., 1984; Serrano et al., 1984). Proteolytically cleaved tubulins that lack carboxy-

† This work was supported in part by American Cancer Society Grants CH-99E and CD-228F to H.S. A preliminary report of several aspects of this study was presented at the June 1983 meeting of the American Society of Biological Chemists.
* Address correspondence to this author.
‡ Case Western Reserve University.
§ Brookhaven National Laboratory.

[1] Abbreviations: PB, microtubule protein stabilizing buffer (pH 6.7) consisting of 0.1 M MES, 2 mM EGTA, 0.1 mM EDTA, 2 mM mercaptoethanol, and 0.5 mM $MgCl_2$; MES, 2-(*N*-morpholino)ethanesulfonic acid; EGTA, ethylene glycol bis(β-aminoethyl ether)-*N*,*N*,*N*',*N*'-tetraacetic acid; EDTA, ethylenediaminetetraacetic acid; MTP, microtubule protein; MAPs, microtubule-associated proteins; HRL, highly reactive lysine; CNBr-HRL, CNBr fragment that contains HRL; PMSF, phenylmethanesulfonyl fluoride; DEP, diethyl pyrocarbonate; $(\alpha/\beta)_{cpm}$, cpm in radiomethylated α-tubulin divided by the corresponding cpm in radiomethylated β-tubulin (α and β subunits obtained from radiomethylated MTP or from radiomethylated PC tubulin electrophoresed on SDS polyacrylamide gels); PC tubulin, phosphocellulose-purified tubulin; SDS, sodium dodecyl sulfate; DTT, dithiothreitol; Tris, tris(hydroxymethyl)aminomethane; PAGE, polyacrylamide gel electrophoresis.

0006-2960/86/0425-4572$01.50/0